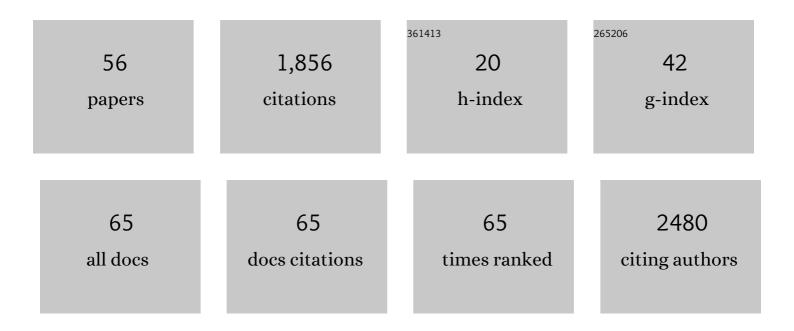


## List of Publications by Year in descending order

Source: https://exaly.com/author-pdf/470997/publications.pdf Version: 2024-02-01



CHAOLI

#	Article	IF	CITATIONS
1	Highly efficient co-sensitization of nanocrystalline TiO2 electrodes with plural organic dyes. New Journal of Chemistry, 2005, 29, 773.	2.8	205
2	Efficient electron injection due to a special adsorbing group's combination of carboxyl and hydroxyl: dye-sensitized solar cells based on new hemicyanine dyes. Journal of Materials Chemistry, 2005, 15, 1654-1661.	6.7	201
3	Trigonal Planar [HgSe <sub>3</sub> ] <sup>4–</sup> Unit: A New Kind of Basic Functional Group in IR Nonlinear Optical Materials with Large Susceptibility and Physicochemical Stability. Journal of the American Chemical Society, 2016, 138, 6135-6138.	13.7	168
4	Direct Observations of Nanofilament Evolution in Switching Processes in HfO <sub>2</sub> â€Based Resistive Random Access Memory by In Situ TEM Studies. Advanced Materials, 2017, 29, 1602976.	21.0	137
5	Photophysical, electrochemical, and photoelectrochemical properties of new azulene-based dye molecules. Journal of Materials Chemistry, 2007, 17, 642-649.	6.7	91
6	In Situ Fully Lightâ€Driven Switching of Superhydrophobic Adhesion. Advanced Functional Materials, 2012, 22, 760-763.	14.9	86
7	PbGa <sub>4</sub> S <sub>7</sub> : a wide-gap nonlinear optical material. Journal of Materials Chemistry C, 2015, 3, 3060-3067.	5.5	80
8	Lunar regolith and substructure at Chang'E-4 landing site in South Pole–Aitken basin. Nature Astronomy, 2021, 5, 25-30.	10.1	61
9	High power, tunable mid-infrared BaGa_4Se_7 optical parametric oscillator pumped by a 21 μm Ho:YAG laser. Optics Express, 2016, 24, 6083.	3.4	57
10	BaGa <sub>2</sub> SnSe <sub>6</sub> : a new phase-matchable IR nonlinear optical material with strong second harmonic generation response. Journal of Materials Chemistry C, 2015, 3, 10998-11004.	5.5	54
11	ESR Signal of Superoxide Radical Anion Adsorbed on TiO2Generated at Room Temperature. Journal of Physical Chemistry B, 2004, 108, 2781-2783.	2.6	51
12	Improved performance in micron-sized silicon anodes by in situ polymerization of acrylic acid-based slurry. Journal of Materials Chemistry A, 2016, 4, 16982-16991.	10.3	47
13	Ba <sub>5</sub> CdGa <sub>6</sub> Se <sub>15</sub> , a congruently-melting infrared nonlinear optical material with strong SHG response. Journal of Materials Chemistry C, 2017, 5, 1057-1063.	5.5	46
14	Effect of surface modification on electrochemical performance of nano-sized Si as an anode material for Li-ion batteries. RSC Advances, 2016, 6, 34715-34723.	3.6	45
15	SnGa <sub>2</sub> GeS <sub>6</sub> : synthesis, structure, linear and nonlinear optical properties. Dalton Transactions, 2015, 44, 7404-7410.	3.3	40
16	Noncentrosymmetric chalcogenides BaZnSiSe4 and BaZnGeSe4 featuring one-dimensional structures. Journal of Alloys and Compounds, 2017, 708, 414-421.	5.5	39
17	Dynamic observation of oxygen vacancies in hafnia layer by in situ transmission electron microscopy. Nano Research, 2015, 8, 3571-3579.	10.4	37
18	Be <sub>2</sub> BO <sub>3</sub> F: A Phase of Beryllium Fluoride Borate Derived from KBe <sub>2</sub> BO <sub>3</sub> F <sub>2</sub> with Short UV Absorption Edge. Inorganic Chemistry, 2016, 55, 6586-6591.	4.0	36

Chao Li

#	Article	IF	CITATIONS
19	K <sub>2</sub> Sn <sub>2</sub> ZnSe <sub>6</sub> , Na <sub>2</sub> Ge <sub>2</sub> ZnSe <sub>6</sub> , and Na <sub>2</sub> In <sub>2</sub> GeSe <sub>6</sub> : a new series of quaternary selenides with intriguing structural diversity and nonlinear optical properties. Dalton Transactions, 2016, 45, 7627-7633.	3.3	32
20	DNA photocleavage in anaerobic conditions by a Ru(ii) polypyridyl complex with long wavelength MLCT absorption. New Journal of Chemistry, 2010, 34, 137-140.	2.8	23
21	High-pulse-energy mid-infrared optical parametric oscillator based on BaGa4Se7 crystal pumped at 1.064Aî¼m. Applied Physics B: Lasers and Optics, 2017, 123, 1.	2.2	20
22	Temperature-Dependent Sellmeier Equations of IR Nonlinear Optical Crystal BaGa4Se7. Crystals, 2017, 7, 62.	2.2	18
23	Fluorination on non-photolabile dppz ligands for improving Ru( <scp>ii</scp> ) complex-based photoactivated chemotherapy. Dalton Transactions, 2019, 48, 12177-12185.	3.3	18
24	Four new chalcohalides, NaBa2SnS4Cl, KBa2SnS4Cl, KBa2SnS4Br and CsBa2SnS4Cl: Syntheses, crystal structures and optical properties. Journal of Solid State Chemistry, 2015, 227, 104-109.	2.9	17
25	A polypyridyl Co( <scp>ii</scp> ) complex-based water reduction catalyst with double H <sub>2</sub> evolution sites. Catalysis Science and Technology, 2016, 6, 8482-8489.	4.1	16
26	Smart use of "ping-pong―energy transfer to improve the two-photon photodynamic activity of an Ir( <scp>iii</scp> ) complex. Chemical Communications, 2020, 56, 2845-2848.	4.1	16
27	The Double Molybdate Rb <sub>2</sub> Ba(MoO <sub>4</sub> ) <sub>2</sub> : Synthesis, Crystal Structure, Optical, Thermal, Vibrational Properties, and Electronic Structure. Zeitschrift Fur Anorganische Und Allgemeine Chemie, 2015, 641, 2321-2325.	1.2	14
28	Sn2SiS4, synthesis, structure, optical and electronic properties. Optical Materials, 2015, 47, 379-385.	3.6	14
29	Eliminating above-surface diffractions from ground-penetrating radar data using iterative Stolt migration. Geophysics, 2021, 86, H1-H11.	2.6	14
30	Syntheses, crystal structures and physical properties of three new chalcogenides: NaGaGe <sub>3</sub> Se <sub>8</sub> , K <sub>3</sub> Ga <sub>3</sub> Ge <sub>7</sub> S <sub>20</sub> , and K <sub>3</sub> Ga <sub>3</sub> Ge <sub>7</sub> Se <sub>20</sub> . Dalton Transactions, 2016, 45, 532-538.	3.3	13
31	Velocity Analysis Using Separated Diffractions for Lunar Penetrating Radar Obtained by Yutu-2 Rover. Remote Sensing, 2021, 13, 1387.	4.0	13
32	Li <sub>2</sub> MnSnSe <sub>4</sub> : A New Quaternary Diamondâ€Like Semiconductor with Nonlinear Optical Response and Antiferromagnetic Property. Chemistry - an Asian Journal, 2017, 12, 3172-3177.	3.3	12
33	Photo-induced mitochondrial DNA damage and NADH depletion by –NO <sub>2</sub> modified Ru( <scp>ii</scp> ) complexes. Chemical Communications, 2021, 57, 4162-4165.	4.1	11
34	Selective and Efficient Photoinactivation of Intracellular Staphylococcus aureus and MRSA with Little Accumulation of Drug Resistance: Application of a Ru(II) Complex with Photolabile Ligands. Journal of Medicinal Chemistry, 2021, 64, 7359-7370.	6.4	11
35	Energetic transients joint analysis system for multi-INstrument (ETJASMIN) for GECAM – I. Positional, temporal, and spectral analyses. Monthly Notices of the Royal Astronomical Society, 2022, 514, 2397-2406.	4.4	11
36	Rock Location and Property Analysis of Lunar Regolith at Chang'E-4 Landing Site Based on Local Correlation and Semblance Analysis. Remote Sensing, 2021, 13, 48.	4.0	10

Chao Li

#	Article	IF	CITATIONS
37	Quaternary chalcogenides BaRE <sub>2</sub> In <sub>2</sub> Ch <sub>7</sub> (RE = La–Nd; Ch = S, Se) containing InCh <sub>5</sub> trigonal bipyramids. Dalton Transactions, 2016, 45, 12329-12337.	3.3	8
38	A Ru(II)â€Based Nanoassembly Exhibiting Theranostic PACT Activity in NIR Region. Particle and Particle Systems Characterization, 2020, 37, 2000045.	2.3	8
39	para-Dialkylaminophenyl Dyes for Efficient Nanocrystalline TiO2 Sensitization in Far-red Region. Chinese Journal of Chemistry, 2006, 24, 537-545.	4.9	7
40	Recent Progress of HTS Microwave Applications in Satellite Receiver, Meteorological Radar, Mobile Communication and Radio Astronomy. Journal of Superconductivity and Novel Magnetism, 2013, 26, 1843-1848.	1.8	7
41	Ba <sub>3</sub> FeS <sub>4</sub> Br: A 0D Ironâ€Based Chalcohalide with Unusual Magnetic Properties. European Journal of Inorganic Chemistry, 2016, 2016, 1359-1363.	2.0	7
42	Application of the Organic Photosensitizers Bearing Two Carboxylic Acid Groups to Dyeâ€ <del>S</del> ensitized Solar Cells. Chinese Journal of Chemistry, 2008, 26, 929-934.	4.9	6
43	Noncentrosymmetric selenide Ba4Ga4GeSe12: Synthesis, structure, and optical properties. Journal of Solid State Chemistry, 2016, 241, 131-136.	2.9	6
44	Li <sub>7</sub> Cd <sub>4.5</sub> Ge <sub>4</sub> Se <sub>16</sub> and Li <sub>6.4</sub> Cd <sub>4.8</sub> Sn <sub>4</sub> Se <sub>16</sub> : Strong Nonlinear Optical Response in Quaternary Diamondâ€Like Selenide Networks. Chemistry - an Asian Journal, 2018, 13, 871-876.	3.3	6
45	When one becomes two: Ba12In4Se20, not quite isostructural to Ba12In4S19. Journal of Solid State Chemistry, 2017, 253, 29-34.	2.9	5
46	Optical characterization of GaN/AlGaN bilayer by transmission and reflection spectra. Journal of Applied Physics, 2010, 108, 063104.	2.5	4
47	Development of an L-Band HTS Duplexer Sub-system with Novel Stepped Impedance Resonators. Journal of Superconductivity and Novel Magnetism, 2013, 26, 1849-1852.	1.8	4
48	The structural transitions of C <sub>60</sub> nanowhiskers under an electric field characterized by in situ transmission electron microscopy and electron energy-loss spectroscopy. Nanoscale, 2014, 6, 6585-6589.	5.6	4
49	Wavefield separation using irreversible-migration filtering. Geophysics, 2022, 87, A43-A48.	2.6	4
50	A VHF band HTS filter based on modified single-spiral resonators for radio astronomy application. Science China: Physics, Mechanics and Astronomy, 2013, 56, 910-915.	5.1	3
51	Chloromethyl-modified Ru( <scp>ii</scp> ) complexes enabling large pH jumps at low concentrations through photoinduced hydrolysis. Chemical Science, 2019, 10, 9949-9953.	7.4	3
52	Ca2SnS4: Crystal structure, optical property, and electronic structure. Journal of Crystal Growth, 2016, 434, 67-71.	1.5	2
53	Structure resonance crossing in space charge dominated beams. Physics of Plasmas, 2019, 26, 053104.	1.9	1
54	Preserving signal during random noise attenuation through migration enhancement and local orthogonalization. Geophysics, 2022, 87, V451-V466.	2.6	1

Chao Li

#	Article	IF	CITATIONS
55	Converting an Almost Noncytotoxic Ru(II) Complex with Photolabile Ligands into a Highly Efficient PACT Agent. Particle and Particle Systems Characterization, 2021, 38, 2100193.	2.3	Ο
56	Separating Scholte Wave and Body Wave in OBN Data Using Wave-Equation Migration. IEEE Transactions on Geoscience and Remote Sensing, 2022, 60, 1-13.	6.3	0